

## Kapitza Trap for Ultracold Atoms

Jian Jiang, Erik Bernhart<sup>✉</sup>, Marvin Röhrle<sup>✉</sup>, Jens Benary<sup>✉</sup>, Marvin Beck<sup>✉</sup>,

Christian Baals<sup>✉</sup>, and Herwig Ott<sup>✉\*</sup>

*Department of Physics and Research Center OPTIMAS, Technische Universität Kaiserslautern,  
67663 Kaiserslautern, Germany*

 (Received 22 December 2021; revised 21 November 2022; accepted 9 June 2023; published 20 July 2023)

We report on the experimental realization of a Kapitza trap for ultracold atoms. Using time-periodic attractive and repulsive Gaussian potentials, we create an effective trap for ultracold neutral atoms in a regime where the time average of the potential is equal to zero. We analyze the role of experimental imperfections, the stability of the trapped atomic cloud, and the magnitude of the effective potential. We find good agreement with the high-frequency expansion of the underlying system dynamics. Our experimental approach opens up new possibilities to study Floquet systems of neutral atoms.

DOI: [10.1103/PhysRevLett.131.033401](https://doi.org/10.1103/PhysRevLett.131.033401)

Manipulating states and dynamics of a system by periodic driving is known as Floquet engineering [1,2], which is increasingly employed in many areas of physics, including cold atoms [3], photonics [4], and solid-state physics [5]. By designing suitable periodic driving, one can engineer an effective time-independent Hamiltonian with properties that are otherwise not attainable in the corresponding static system. Kapitza's pendulum [6,7], an inverted pendulum that is dynamically stabilized by a fast driving of its pivot point, is the most prominent example of such engineering in classical physics. Many applications of Kapitza stabilization in quantum systems have been proposed, including the breaking of translation symmetry [8], the periodically driven sine-Gordon model [9], the stabilization of bright solitons in a Bose-Einstein condensate (BEC) [10], cold atoms with oscillating interactions [11], optical molasses [12], preparation of molecular ions [13], the stability of optical resonators [14], polariton Rabi oscillation [15], and unconventional dynamical phases [16]. In particular, Kapitza stabilization can be employed to trap particles. The most notable example of such an application is the Paul trap [17,18], where a saddle point potential is modulated periodically to create a confining harmonic potential. Light confinement in dielectric structures with a transverse refractive index distribution periodically modulated in the longitudinal coordinate has been proposed [19] and experimentally demonstrated [20]. Regarding trapping atoms by laser fields, Ref. [21] has proposed and analyzed how a spatially oscillating red-detuned optical lattice could localize a repulsively interacting BEC, and Ref. [22] has investigated the case where a time-periodic localized attractive and repulsive Gaussian potential with a vanishing time average creates a conservative trapping potential.

In this Letter, inspired by the theoretical work in Ref. [22], we demonstrate a “Kapitza trap” for ultracold

atoms and thereby extend the field of Kapitza pendulum physics toward the regime of ultracold quantum gases. The Kapitza trap is created by superimposing time-modulated focused laser beams to induce a time-varying dipole trapping potential for neutral atoms.

Specifically, we confine ultracold <sup>87</sup>Rb atoms using a time-periodic Gaussian potential of the form [Fig. 1(a)]

$$V_t(r, t) = V_0 \exp\left(-\frac{2r^2}{\sigma^2}\right) \cos(\omega t), \quad (1)$$

where  $\sigma$  and  $V_0$  are the waist and amplitude of the Gaussian profile, respectively, and  $r = (x^2 + y^2)^{1/2}$  is the radial coordinate. In practice,  $V_t$  is the result of the superposition of a repulsive potential,

$$V_b(r, t) = V_{b0} \exp\left(-\frac{2r^2}{\sigma_b^2}\right) \frac{1 + \cos(\omega t)}{2} \quad (2)$$

$$= G_b(r)[1 + \cos(\omega t)]/2, \quad (3)$$

and an attractive potential,

$$V_r(r, t) = V_{r0} \exp\left(-\frac{2r^2}{\sigma_r^2}\right) \frac{1 - \cos(\omega t)}{2} \quad (4)$$

$$= G_r(r)[1 - \cos(\omega t)]/2, \quad (5)$$

created by a blue-detuned laser (777.827 nm) and a red-detuned laser (782.325 nm) [23]. These two lasers are referred to as Kapitza lasers. In Eqs. (3) and (5), we have introduced  $G_b$  and  $G_r$  to represent their unmodulated Gaussian profiles. For equal power, the two laser beams induce dipole potentials with the same magnitude but opposite sign for <sup>87</sup>Rb, i.e.,  $V_{b0} = -V_{r0} = V_0$ . Both lasers

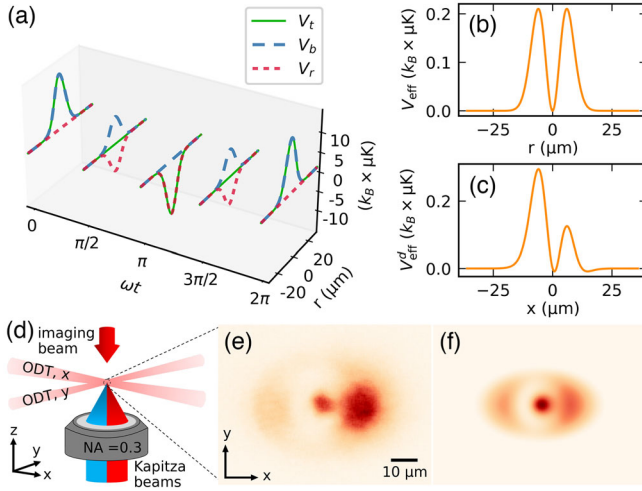


FIG. 1. Working principle of the Kapitza trap. Kapitza laser: waist  $\sigma = 12 \mu\text{m}$ , amplitude  $V_0 = k_B \times 14 \mu\text{K}$ , modulation frequency  $\omega/2\pi = 2.4 \text{ kHz}$ . (a) Time-modulated Gaussian potential  $V_t$  for one oscillation period.  $V_b$  and  $V_r$  are the individual potentials of the two Kapitza lasers. (b) Effective potential  $V_{\text{eff}}$  in the high-frequency limit [Eq. (6)]. The distance between the two peaks is  $\sigma$ . (c) Effective potential  $V_{\text{eff}}^d$  at  $y = 0$  for a small displacement of  $d = 120 \text{ nm}$  between the two laser beams [Eq. (8)]. (d) Experimental setup. (e) Absorption image of the atomic cloud in the Kapitza trap. (f) Calculated atomic density plotted with the same coordinate and length scale of (e). Densities in both cases are rescaled from 0 to 1, where 1 is the maximum density in each individual case.

have the same linear polarization, but their power modulation is out of phase by  $180^\circ$ . In order to ensure maximum spatial overlap and equal waists ( $\sigma_b = \sigma_r = \sigma$ ) of the two beams at the position of the atoms, we couple both lasers into the same polarization-maintaining single-mode fiber. The resulting effective potential  $V_{\text{eff}}$  in the high-frequency limit then reads to first order [22,26] [Fig. 1(b)],

$$V_{\text{eff}}(r) = \frac{4V_0^2}{m\sigma^4\omega^2} r^2 \exp\left(-\frac{4r^2}{\sigma^2}\right), \quad (6)$$

where  $m$  is the mass of a trapped atom. Applying the harmonic approximation to  $V_{\text{eff}}$  at  $r = 0$ , we derive the oscillation frequency  $\Omega = 2\sqrt{2}V_0/m\sigma^2\omega$  of an atom in the Kapitza trap. Equation (6) is a good approximation for  $\omega \gg \Omega$  [22]. Because  $V_{\text{eff}}$  stems from the mean kinetic energy stored in the micromotion of the particles, it is always positive and peaks at maxima of the kinetic energy of the particle's micromotion. The same microscopic dynamics is also responsible for the effective potential of a Paul trap.

The two maxima of  $V_{\text{eff}}$ ,  $V_{\text{eff}}^{\text{max}} = V_{\text{eff}}(r = \pm\sigma/2)$ , are separated by the waist of the Kapitza beam  $\sigma$ . Note that in order to create the same trapping potential exclusively using lasers without time modulation, one requires a waist

that is smaller by a factor of  $\sqrt{2}$ . While more subtle methods [27,28] are available for creating optical potentials with even better resolutions, our approach is, at least in principle, a straightforward way to surpass the diffraction limit modestly.

The experimental setup is sketched in Fig. 1(d). We start by producing a BEC of  $^{87}\text{Rb}$  atoms confined in a crossed optical dipole trap (ODT,  $\lambda = 1064 \text{ nm}$ ). The trap frequencies are  $\omega_x/2\pi = 55 \text{ Hz}$ ,  $\omega_y/2\pi = 93 \text{ Hz}$ , and  $\omega_z/2\pi = 108 \text{ Hz}$ , where the  $z$  direction is antiparallel to the direction of gravity. The central chemical potential of the condensate is  $\mu \approx k_B \times 300 \text{ nK}$ . The Kapitza lasers, which are focused on the condensate along the  $z$  direction by an objective with a numerical aperture (NA) of 0.3, are then linearly ramped up [29] and held until the system is probed by *in situ* absorption imaging using the same objective. Power modulation of the Kapitza lasers is always on during the ramp and the hold time. Since the dominant confinement along the  $z$  direction is from the ODT, the total trapping potential is well approximated by the two-dimensional Kapitza trap in the radial direction [Eq. (6)] and the superimposed ODT.

In Fig. 1(e), we show a typical absorption image of the trapped atomic cloud with Kapitza beams whose waists are  $12 \mu\text{m}$ . The Kapitza trap in the center is clearly visible and demonstrates the basic working principle. The annular depletion zone between the Kapitza trap and the outer ring of atoms is a direct consequence of the rotationally symmetric effective potential, which creates a ring barrier.

Although both Kapitza beams share the same spatial mode, the different wavelength is likely to cause a slight displacement between their beam profiles via dispersive optical elements. Because of the displacement, the Kapitza trap is always closer to the right side of the outer ring, where the atomic density is higher than the rest of the ring. To quantitatively analyze this phenomenon, we introduce a displacement  $d$  along the  $x$  axis of the red-detuned beam:

$$G_r(x, y, d) = V_{r0} \exp\left(-\frac{(x-d)^2 + y^2}{\sigma_r^2/2}\right). \quad (7)$$

The effective potential can then be written as [26]

$$\begin{aligned} V_{\text{eff}}^d(x, y, d) &= \frac{G_b + G_r}{2} + \frac{1}{m\sigma^4\omega^2} \{(x^2 + y^2)G_b^2 \\ &\quad + 2[x(x-d) + y^2]G_bG_r \\ &\quad + [(x-d)^2 + y^2]G_r^2\} \\ &\equiv V_{\text{res}} + V_K, \end{aligned} \quad (8)$$

where  $V_{\text{res}}$  is the residual potential induced by the displacement and  $V_K$  is the potential of the Kapitza trap, a ring barrier potential similar to  $V_{\text{eff}}$  but not centered at the coordinate origin when  $d \neq 0$ . According to Eq. (8), a small displacement of  $120 \text{ nm}$  is already sufficient to imbalance

the Kapitza trap [Fig. 1(c)]. For  $d > 240$  nm, which amounts to only 2% of the beam waist, the trap disappears as  $V_{\text{res}}$  dominates. We determine the displacement as 120 nm (corresponding to  $0.01 \times \sigma$  by comparing the experimental result and the calculated atomic density [23], which is given by the time-independent Gross-Pitaevskii equation in Thomas-Fermi approximation). Figure 1(f) shows the reconstructed density for  $V_{\text{eff}}^d(x, y, d = 120 \text{ nm})$  and a chemical potential of  $\mu_d = k_B \times 400$  nK. This model captures most of the features observed in the experiment, including the asymmetry of the cloud.

Similar to the spatial displacement, any other imperfect alignment (e.g., power imbalance, beam waist mismatch) of the two Kapitza beams will result in a finite  $V_{\text{res}}$ . The maximum of  $V_K$  has the same order of magnitude as  $V_{\text{eff}}^{\text{max}}$ . From Eq. (6), one can deduce that  $V_0/V_{\text{eff}}^{\text{max}} = (2\sqrt{2}e)(\omega/\Omega) \simeq 8\omega/\Omega$ . In the experiment shown in Fig. 1(e), we have  $\omega/\Omega = 9$ , which corresponds to  $V_0/V_{\text{eff}}^{\text{max}} \simeq 72$ . Such conditions require that  $V_{\text{res}}$  is about 2 orders of magnitude smaller than  $V_0$  in order to observe the Kapitza trap. This can only be achieved by a careful alignment of the two laser beams. In the experiment, we change the relative power of the two beams in subpercent steps until the Kapitza trap appears together with the outer ring. We refer to this as the balanced situation, going away from which the feature disappears already for a few percent beam imbalance.

It is instructive to compare the Kapitza trap for neutral atoms with the Paul trap for charged particles. While the electric field couples directly to the charge of the particles, neutral atoms couple via their polarizability to the light field. Accordingly, the later coupling is orders of magnitude weaker, so realizing a Kapitza trap for neutral atoms is much more challenging. On the other hand, a maximum of the light field can easily be created in free space. Thus, in principle, the Kapitza trap provides a way to confine neutral atoms in all three spatial dimensions by oscillating optical potentials alone without requiring close-by electrodes as in a Paul trap.

We now turn to the stability analysis and characteristics of the Kapitza trap. In the high-frequency limit,  $V_{\text{eff}}$  remains constant when proportionally increasing  $V_0$  and  $\omega$  [Eq. (6)]. Hence, the trap frequency  $\Omega$  also remains unaffected. The ratio  $\omega/\Omega$ , however, increases. This way, we can test the system behavior in the high- and low-frequency limits by measuring the lifetime of the trapped atoms. This works, however, only in a limited parameter range for a given displacement. While  $V_K$  will remain unchanged,  $V_{\text{res}}$  will increase monotonously and therefore become dominant. In other words, a given displacement sets an upper limit for  $\omega/\Omega$  in such a test. The highest  $\omega/\Omega$  we achieve for a beam waist of 12  $\mu\text{m}$  is about 9 [Fig. 1(e)].

Figure 2(a) shows the measured lifetimes of atoms inside the Kapitza trap ( $\tau_K$ ) and the outer ring ( $\tau_c$ ) as  $V_0$  and  $\omega$  increase proportionally, keeping  $\Omega$  approximately

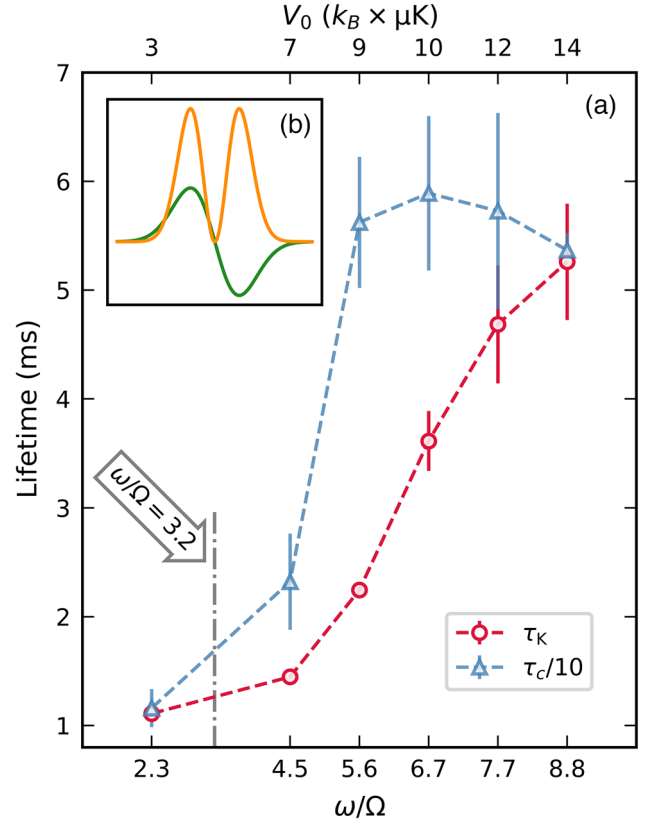


FIG. 2. (a) Lifetimes of atoms inside the Kapitza trap ( $\tau_K$ ) and the outer ring ( $\tau_c$ , scaled down by a factor of 10) dependent on the modulation frequency  $\omega$  for approximately constant  $\Omega$ , plotted against  $\omega/\Omega$ . To determine the number of atoms in the Kapitza trap, we integrate the atomic density over a circle with a diameter of  $2\sigma/3$  [8  $\mu\text{m}$ ; see also Fig. 1(b)]. The upper axis shows the potential  $V_0$ , which is increased proportional to  $\omega$ . Data points are connected by dashed lines for better visualization. (b)  $V_{\text{res}}$  (green line) and  $V_K$  (orange line) at  $\omega/\Omega = 8.8$ , plotted with the same scale.

constant [30]. Equation (6) becomes a more accurate approximation for increasing modulation frequency  $\omega$ . At the same time, the excitation of the atomic motion is expected to become less pronounced as the time-varying potential couples less efficiently to the atoms at higher frequencies. The above trends are clearly observed in our experiment as measured lifetimes,  $\tau_K$  and  $\tau_c$ , increase with the modulation frequencies. On the other hand,  $\tau_K$  is still strongly affected by the time-periodic potential even at high frequencies, and it is at least one order of magnitude smaller than  $\tau_c$  for the same  $\omega/\Omega$ . This can be attributed to several effects. As shown in Fig. 2(b),  $V_{\text{res}}$  resulting from the beam displacement pushes atoms away from the trap center. These atoms move in an area with larger oscillating potential, which leads to additional heating because the energy of the micromotion can be converted into the energy of the macromotion. This phenomenon can be analogized to the well-known excess micromotion of charged particles in a Paul trap without proper dc compensation voltages [31].

Collisions between atoms intensify such a heating process [32]. Light scattering from the Kapitza beams, unstable orbits due to the nonparabolic central well structure of the effective potential, and three-body losses constitute additional heating and loss processes, which further reduce the lifetime.

The stability of the Kapitza trap can also be analyzed in terms of the classical equation of motion for the atoms in the trap. Approximating the center of the Kapitza trap with a harmonic trap, the equation of motion can be written as

$$\frac{d^2x}{d\tau^2} - 2q \cos(2\tau)x = 0, \quad (9)$$

where  $\tau = \omega t/2$  and

$$q = \frac{8V_0}{m\sigma^2\omega^2} = \frac{2\sqrt{2}}{\omega/\Omega}. \quad (10)$$

Equation (9) is a standard Mathieu differential equation. For  $q \leq 0.9$ , i.e.,  $\omega/\Omega \geq 3.2$ , this equation has a periodic solution, which implies that the atoms undergo closed orbits and are therefore trapped [33]. In other words, when considering the single-particle picture,  $V_t$  can be replaced by  $V_{\text{eff}}$  for  $\omega/\Omega \geq 3.2$ .

For values of  $\omega/\Omega$  larger than 5,  $\tau_c$  is roughly on a plateau. Without the Kapitza beams, the atomic density amounts to  $3 \times 10^{14} \text{ cm}^{-3}$  in the trap center, corresponding to a lifetime of 2 s. When switched on, the Kapitza trap compresses the outer ring of atoms due to the effective repulsion and leads to enhanced three-body losses. As they depend on  $V_0$  (see Fig. 4), which changes slightly for  $\omega/\Omega > 5$ , one would expect  $\tau_c$  are roughly on a plateau. Furthermore, the measured lifetime of several tens of milliseconds could be realistic, if one takes into account that noncondensed atoms have a sixfold higher three-body loss rate compared to Bose-condensed atoms [34].

To understand the effect of the beam size on the Kapitza trap, we have also performed experiments with smaller Kapitza beams ( $\sigma = 6 \mu\text{m}$ ). We first note that the Kapitza trap is no longer visible in the absorption images, which is most likely due to a more significant relative displacement of both beams. However, we observe the appearance of a hole in the density distribution as a signature of the time-modulated potential. The effective potential can be estimated by analyzing the characteristics of this hole. Figure 3(a) shows the appearance of the hole when the modulation frequency decreases. At very high modulation frequencies, the effective potential is negligible compared to the chemical potential of the condensate, and only a minor effect is visible. As the modulation frequency decreases, a hole starts to show up at the center of the cloud when the effective potential becomes comparable with the chemical potential. At small modulation frequencies, the effective potential is no longer a good

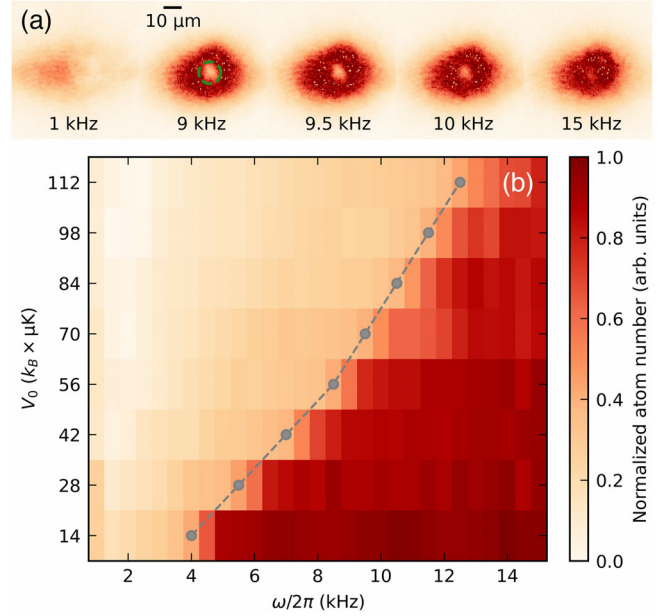


FIG. 3. (a) Appearance of a hole in the atomic cloud upon applying the Kapitza lasers ( $\sigma = 6 \mu\text{m}$ ,  $V_0 = 70 \mu\text{K}$ ). The dashed green circle defines the hole area, in which we determine the number of expelled atoms. (b) Atom number inside the hole area. Measured atom numbers are normalized to the maximum number of atoms measured inside the green circle. Gray points (with dashed line as a guide to the eye) represent  $(V_0, \omega/2\pi)$  for forming evident holes.

approximation, and the small frequency perturbations strongly affect the cloud.

For a quantitative evaluation, we take images of the cloud for different combinations of the Kapitza lasers' powers and modulation frequencies, and determine the number of atoms inside the hole area [green dashed circle in Fig. 3(a)]. The result is shown in Fig. 3(b). We observe that there is a frequency above which the hole disappears for each power level. The transition is rather steep. In order to provide a theoretical estimate for the creation of the hole, we proceed as follows. The effective potential leads to a spatially varying reduction of the density. Averaging the effective potential in the transverse direction over an area  $A$  gives  $V_{\text{av}} = A^{-1} \iint dx dy V_{\text{eff}}^d(x, y, d)$ . We chose  $\sigma/\sqrt{2}$  as the radius for the area. An evident hole is then formed, when this averaged potential is equal to the chemical potential of the atoms. These points are shown as gray dots in Fig. 3(b). The quantitative agreement confirms that the effective potential is a good description for this parameter range.

We measure the lifetime  $\tau'_c$  of the whole atomic cloud to investigate further the validity of the effective potential approximation for the smaller Kapitza beams. The result is plotted as  $1/\tau'_c$  against  $\omega/\Omega$  (Fig. 4) for better visualization. As one would expect,  $\tau'_c$  has a similar behavior as  $\tau_c$ . It first increases and then reaches a plateau beyond a specific  $\omega/\Omega$ . For larger  $V_0$ , the compression of the atomic cloud

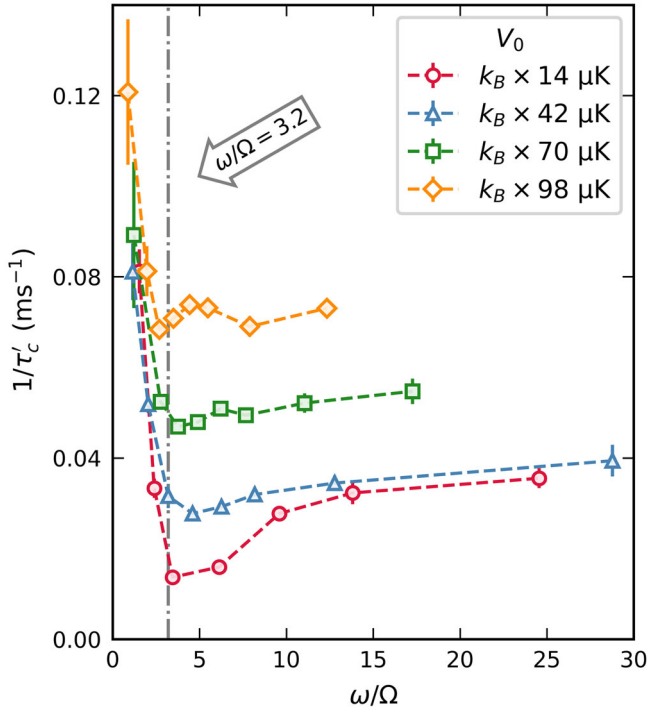


FIG. 4. Lifetime ( $\tau'_c$ ) of the whole atomic cloud in the presence of the Kapitza beams for different strengths. For  $\omega/\Omega > 3.2$ ,  $\tau'_c$  is roughly a constant. Dashed lines are guides to the eye.

caused by the repulsion of the effective potential is stronger. Therefore, the corresponding  $\tau'_c$  on the plateau is smaller.

In summary, we have experimentally demonstrated a Kapitza trap for ultracold atoms. Employing a rapid time-periodic Gaussian potential, realized with red- and blue-detuned focused laser beams, we confine ultracold  $^{87}\text{Rb}$  atoms with an effective ring barrier potential. We validate the approximation of the effective potential in the high-frequency limit. At present, our trapped samples suffer from limited lifetimes, limited achievable modulation frequency, and residual static potentials due to relative beam displacement. Further eliminating this 1% beam displacement is the key to verifying and sorting out these issues. We suspect the in-vacuum objective used in this experiment induces the displacement since it is designed for monochromatic light. In principle, exclusively using reflective optics after the fiber employed for overlapping the Kapitza beams can avoid chromatic aberration so that the two beams fully overlap and have the same size at the position of the atoms.

Once the lifetime of the atoms in the Kapitza trap is increased, our approach allows for various new research directions. First, we recall that the effective potential exhibits a tunneling barrier. This feature allows for studying quantum tunneling in time-periodic potentials, where the tunneling rate can be reduced or even completely suppressed [35–37]. A further extension of our work is the detailed study of the low-frequency limit. This is the realm

of resonant Floquet systems, where the modulation frequency matches an intrinsic frequency of the system. Such driving has been proposed, for instance, to implement energy and spin filters [38,39] and has recently been extended to interacting systems [40]. Because of the Gaussian envelope of the time-periodic potential  $V_t$  [Eq. (1)], our system is intrinsically nonlinear. This makes it also a potential tool for investigating chaos in the classical and quantum regime [41].

We gratefully acknowledge discussions with Ido Gilary, Serena Fazzini, and Junhui Zheng. We acknowledge financial support by the Deutsche Forschungsgemeinschaft within the Forschungsgroßgeräteprogramm INST 248/250-1 and the collaborative research center TRR 185, Project B3 (No. 277625399).

\*ott@physik.uni-kl.de

- [1] C. Weitenberg and J. Simonet, Tailoring quantum gases by Floquet engineering, *Nat. Phys.* **17**, 1342 (2021).
- [2] M. Bukov, L. D'Alessio, and A. Polkovnikov, Universal high-frequency behavior of periodically driven systems: from dynamical stabilization to Floquet engineering, *Adv. Phys.* **64**, 139 (2015).
- [3] A. Eckardt, Atomic quantum gases in periodically driven optical lattices, *Rev. Mod. Phys.* **89**, 011004 (2017).
- [4] T. Ozawa, H. M. Price, A. Amo, N. Goldman, M. Hafezi, L. Lu, M. C. Rechtsman, D. Schuster, J. Simon, O. Zilberberg, and I. Carusotto, Topological photonics, *Rev. Mod. Phys.* **91**, 015006 (2019).
- [5] T. Oka and S. Kitamura, Floquet engineering of quantum materials, *Annu. Rev. Condens. Matter Phys.* **10**, 387 (2019).
- [6] P.L. Kapitza, Dynamic stability of the pendulum with vibrating suspension point, *Usp. Fiz. Nauk* **44**, 7 (1951); [*Sov. Phys. JETP* **21**, 488 (1951)].
- [7] L. D. Landau and E. M. Lifshitz, *Mechanics* (Pergamon Press, Oxford, 1976).
- [8] S. V. Rajagopal, K. M. Fujiwara, R. Senaratne, K. Singh, Z. A. Geiger, and D. M. Weld, Quantum emulation of extreme non-equilibrium phenomena with trapped atoms, *Ann. Phys. (Berlin)* **529**, 1700008 (2017).
- [9] R. Citro, E. G. Dalla Torre, L. D'Alessio, A. Polkovnikov, M. Babadi, T. Oka, and E. Demler, Dynamical stability of a many-body Kapitza pendulum, *Ann. Phys. (Amsterdam)* **360**, 694 (2015).
- [10] F. K. Abdullaev and R. Galimzyanov, The dynamics of bright matter wave solitons in a quasi one-dimensional Bose–Einstein condensate with a rapidly varying trap, *J. Phys. B* **36**, 1099 (2003).
- [11] F. K. Abdullaev, J. G. Caputo, R. A. Kraenkel, and B. A. Malomed, Controlling collapse in Bose–Einstein condensates by temporal modulation of the scattering length, *Phys. Rev. A* **67**, 013605 (2003).
- [12] V. S. Bagnato, N. P. Bigelow, G. I. Surdutovich, and S. C. Zilio, Dynamical stabilization: A new model for supermolasses, *Opt. Lett.* **19**, 1568 (1994).

- [13] O. Smirnova, M. Spanner, and M. Y. Ivanov, Molecule Without Electrons: Binding Bare Nuclei with Strong Laser Fields, *Phys. Rev. Lett.* **90**, 243001 (2003).
- [14] B. T. Torosov, G. Della Valle, and S. Longhi, Imaginary Kapitza pendulum, *Phys. Rev. A* **88**, 052106 (2013).
- [15] N. S. Voronova, A. A. Elistratov, and Y. E. Lozovik, Inverted pendulum state of a polariton Rabi oscillator, *Phys. Rev. B* **94**, 045413 (2016).
- [16] A. Lerose, J. Marino, A. Gambassi, and A. Silva, Prethermal quantum many-body Kapitza phases of periodically driven spin systems, *Phys. Rev. B* **100**, 104306 (2019).
- [17] W. Paul, Electromagnetic traps for charged and neutral particles, *Rev. Mod. Phys.* **62**, 531 (1990).
- [18] N. Goldman and J. Dalibard, Periodically Driven Quantum Systems: Effective Hamiltonians and Engineered Gauge Fields, *Phys. Rev. X* **4**, 031027 (2014).
- [19] A. Alberucci, L. Marrucci, and G. Assanto, Light confinement via periodic modulation of the refractive index, *New J. Phys.* **15**, 083013 (2013).
- [20] A. L. M. Muniz, A. Alberucci, C. P. Jisha, M. Monika, S. Nolte, R. Morandotti, and U. Peschel, Kapitza light guiding in photonic mesh lattice, *Opt. Lett.* **44**, 6013 (2019).
- [21] J. Martin, B. Georgeot, D. Guéry-Odelin, and D. L. Shepelyansky, Kapitza stabilization of a repulsive Bose-Einstein condensate in an oscillating optical lattice, *Phys. Rev. A* **97**, 023607 (2018).
- [22] I. Gilary, N. Moiseyev, S. Rahav, and S. Fishman, Trapping of particles by lasers: The quantum Kapitza pendulum, *J. Phys. A* **36**, L409 (2003).
- [23] See Supplemental Material, which includes Refs. [24,25], at <http://link.aps.org/supplemental/10.1103/PhysRevLett.131.033401> for more details about the wavelength selection of the two Kapitza lasers. While the lasers used to create the Kapitza trap are quite close to the  $D2$  line of  $^{87}\text{Rb}$ , the photon scattering rate in our experiment is in the order of a few Hertz. See Supplemental Material also for the effective potentials and calculated atomic densities for different displacements.
- [24] R. Grimm, M. Weidemüller, and Y. B. Ovchinnikov, Optical dipole traps for neutral atoms, *Adv. At. Mol. Opt. Phys.* **42**, 95 (2000).
- [25] R. H. Leonard, A. J. Fallon, C. A. Sackett, and M. S. Safronova, High-precision measurements of the  $^{87}\text{Rb}$   $D$ -line tune-out wavelength, *Phys. Rev. A* **92**, 052501 (2015).
- [26] S. Rahav, I. Gilary, and S. Fishman, Effective Hamiltonians for periodically driven systems, *Phys. Rev. A* **68**, 013820 (2003).
- [27] W. Ge and M. S. Zubairy, Dark-state optical potential barriers with nanoscale spacing, *Phys. Rev. A* **101**, 023403 (2020).
- [28] Y. Wang, S. Subhankar, P. Bienias, M. Lacki, T.-C. Tsui, M. A. Baranov, A. V. Gorshkov, P. Zoller, J. V. Porto, and S. L. Rolston, Dark State Optical Lattice with a Subwavelength Spatial Structure, *Phys. Rev. Lett.* **120**, 083601 (2018).
- [29] The ramp durations are 3 and 5 ms for experiments using the bigger ( $\sigma = 12 \mu\text{m}$ ) and the smaller ( $\sigma = 6 \mu\text{m}$ ) Kapitza beams, respectively. The hold time for the results shown in Fig. 3(b) is 5 ms.
- [30] Because of the displacement between the two Kapitza beams,  $\Omega$  cannot be a constant. However,  $\Omega$  is treated as a constant since it changes less than 2% during the measurement.
- [31] D. J. Berkeland, J. D. Miller, J. C. Bergquist, W. M. Itano, and D. J. Wineland, Minimization of ion micromotion in a Paul trap, *J. Appl. Phys.* **83**, 5025 (1998).
- [32] R. Blümel, An introduction to chaos in dynamic ion traps, *Phys. Scr.* **1995**, 126 (1995).
- [33] C. Foot, *Atomic Physics* (Oxford University Press, New York, 2005).
- [34] E. A. Burt, R. W. Ghrist, C. J. Myatt, M. J. Holland, E. A. Cornell, and C. E. Wieman, Coherence, Correlations, and Collisions: What One Learns About Bose-Einstein Condensates from Their Decay, *Phys. Rev. Lett.* **79**, 337 (1997).
- [35] F. Grossmann, T. Dittrich, P. Jung, and P. Hänggi, Coherent Destruction of Tunneling, *Phys. Rev. Lett.* **67**, 516 (1991).
- [36] A. Eckardt, C. Weiss, and M. Holthaus, Superfluid-Insulator Transition in a Periodically Driven Optical Lattice, *Phys. Rev. Lett.* **95**, 260404 (2005).
- [37] H. Lignier, C. Sias, D. Ciampini, Y. Singh, A. Zenesini, O. Morsch, and E. Arimondo, Dynamical Control of Matter-Wave Tunneling in Periodic Potentials, *Phys. Rev. Lett.* **99**, 220403 (2007).
- [38] D. Thuberg, E. Muñoz, S. Eggert, and S. A. Reyes, Perfect Spin Filter by Periodic Drive of a Ferromagnetic Quantum Barrier, *Phys. Rev. Lett.* **119**, 267701 (2017).
- [39] S. A. Reyes, D. Thuberg, D. Pérez, C. Dauer, and S. Eggert, Transport through an AC-driven impurity: Fano interference and bound states in the continuum, *New J. Phys.* **19**, 043029 (2017).
- [40] S. Fazzini, P. Chudzinski, C. Dauer, I. Schneider, and S. Eggert, Nonequilibrium Floquet Steady States of Time-Periodic Driven Luttinger Liquids, *Phys. Rev. Lett.* **126**, 243401 (2021).
- [41] L. D'Alessio, Y. Kafri, A. Polkovnikov, and M. Rigol, From quantum chaos and eigenstate thermalization to statistical mechanics and thermodynamics, *Adv. Phys.* **65**, 239 (2016).